ELSEVIER

International Journal of Mass Spectrometry and Ion Processes 159 (1996) 75–80

International Journal of Mass Spectrometry and Ion Processes

Vibrationally resolved photoelectron spectroscopy of AlO^- and AlO_2^-

Sunil R. Desai[b], Hongbin Wu[a], Lai-Sheng Wang[a,b,*]

[a]*Department of Physics, Washington State University, Richland, WA 99352, USA*

[b]*Environmental Molecular Sciences Laboratory, Pacific Northwest National Laboratory, MS K2-14, PO Box 999, Richland, WA 99352, USA*

Received 7 February 1996; accepted 25 March 1996

Abstract

Vibrationally resolved photoelectron spectra of AlO^- and AlO_2^- have been obtained at two photon energies, 3.49 and 4.66 eV. Both the ground and first excited states are observed for AlO. The spectrum of AlO_2^- can only be obtained at the higher photon energy due to the high electron affinity (EA) of AlO_2. The electron affinities of AlO and AlO_2 are measured to be 2.60(1) and 4.23(1) eV, respectively. The rather high EAs for both molecules are consistent with the fact that AlO^- and AlO_2^- anions are closed-shell, isoelectronic with SiO and SiO_2, respectively. The vibrational frequency of the AlO^- anion is observed to be 900 (50) cm^{-1}. The vibrational frequencies and excitation energy obtained for AlO agree well with previous optical measurements. The totally symmetric vibrational frequency is observed to be 750 (40) cm^{-1} for AlO_2 and 680 (60) cm^{-1} for AlO_2^-. The AlO_2 molecule, as well as AlO_2^-, is concluded to have a linear OAlO structure from the spectroscopic information obtained.

Keywords: Vibrationally resolved photoelectron spectra; Electron affinity

1. Introduction

Photodetachment photoelectron spectroscopy (PES) involving size-selected negative cluster ions has been a powerful experimental technique to probe the electronic structure of atomic clusters [1–8]. Very recently, we have shown that this technique can also yield spectroscopic information on novel oxide species traditionally studied in low temperature matrices [9–13]. The photodetachment experiment has one definitive advantage because the species under study is unambiguously identified, while the matrix technique relies on annealing and isotope studies to yield information about molecular identity.

AlO has been extensively studied in both low temperature matrices [14–16] and the gas phase [17,18]. It has also been investigated in several theoretical works [19,20], and its structure and bonding are well understood. AlO^- anion has also been studied in one theoretical work in which the electron affinity (EA) of AlO and the vibrational frequency of AlO^- are calculated [21], but there has been no experimental study on the anion.

AlO_2 has been studied in several matrix experiments [15,16,22,23] and theoretical works [24,25], but there has been no gas phase study. Isomers are supposed to exist for AlO_2 in low temperature matrices. However, there have been conflicting assignments about what is observed in the matrices [16]. The most recent calculations conclude that there are two isomers for AlO_2, a linear OAlO and a cyclic AlO_2, with

* Corresponding author.

PII S0168-1176(96)04443-6

the linear form slightly more favored [25], even though the calculated frequencies have been challenged by the recent matrix experiment [16].

We are interested in small aluminum oxide clusters because of the importance of aluminum oxide both in catalysis as substrate materials and in environmental molecular science as a key component in many minerals. In this paper, we report the first photodetachment PES experiments on AlO^- and AlO_2^-, the smallest in the cluster series that are of interest to us. Beside obtaining the EAs for AlO and AlO_2, we also obtain vibrational and electronic information about the corresponding neutrals. The spectroscopic constants that we observed are in agreement with what is known about AlO. A very high EA is observed for AlO_2, and we establish that both AlO_2^- and AlO_2 are linear.

2. Experimental

The details of the experimental apparatus have been published elsewhere [1] and will only be given briefly, emphasizing the modifications pertinent to the current experiments. Fig. 1 shows a schematic of the apparatus, which is composed of a laser-vaporization cluster source, a modified Wiley–McClaren time-of-flight (TOF) mass spectrometer [26], and a magnetic-bottle TOF electron analyzer [5,27]. A pulsed laser beam (532 nm, 10–20 mJ) (2) is focused down to about 1 mm diameter onto a pure aluminum target, producing a plasma containing aluminum atoms in both charged and neutral states. A helium carrier gas, seeded with 0.5% O_2 and delivered by two pulsed molecular beam valves, is mixed with the plasma. The reactions between the aluminum atoms and the oxygen produce the desired $Al_xO_y^-$ clusters. The helium carrier gas and the oxide clusters undergo a supersonic expansion (1), forming a cold and collimated molecular beam by a skimmer. The negative clusters are extracted at 90° from the beam and subjected to a time-of-flight mass analysis (3). The AlO^- or AlO_2^- species are selected by a mass gate (4) and decelerated (5) before photodetachment by a pulsed laser beam (8). The detachment laser beam from a Nd:YAG laser (355 nm or 266 nm) is not focused and has a 5 mm diameter spot size in the detachment zone defined by an aperture outside the vacuum chamber. Typically, a pulse energy between 0.5–3 mJ is used. A higher pulse energy is used at 355 nm to obtain a stronger photoelectron signal. Lower pulse energies are used at 266 nm to reduce the low energy electron noises resulted from scattered photons interacting with the surfaces near the detachment zone.

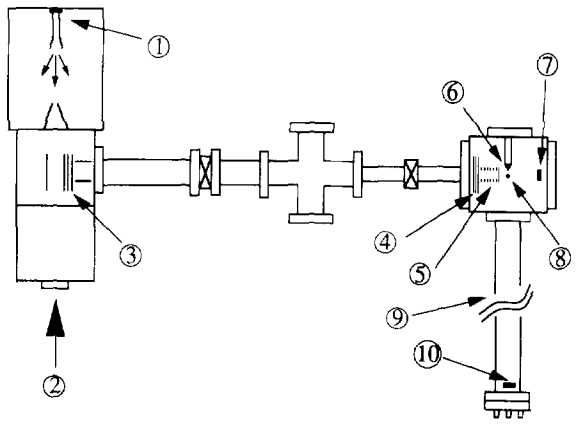

Fig. 1. Schematics of the magnetic-bottle time-of-flight photoelectron spectroscopic apparatus. (1) target and cluster nozzle assembly, (2) vaporization laser beam, (3) ion extraction for time-of-flight mass analysis, (4) three-grid mass gate, (5) momentum cluster ion decelerator, (6) conical iron pole piece and magnet holder, (7) microchannel plates ion detector, (8) detachment laser beam, perpendicular to the paper, (9) 3.5 meter long electron time-of-flight tube, (10) Z-stack microchannel plate array for fast electron detection.

The photoelectrons emitted at all angles are parallelized into the TOF tube (9) by a diverging magnetic field in the interaction zone and detected by an array of microchannel plates (10). A permanent magnet mounted outside the vacuum chamber and a conical iron pole piece mounted inside the chamber (6) generate the required diverging magnetic field and form the magnetic bottle. The 355 nm spectra are taken at 10 Hz repetition rate while the 266 nm spectra are

taken at 20 Hz with the vaporization laser off at alternating shots for background subtraction. The current version of the spectrometer using the permanent magnet configuration has an energy resolution ranging from 20 to 30 meV at 1 eV electron kinetic energy. The best resolution is achieved directly after a fresh bake of the spectrometer and deteriorates somewhat with time, mostly caused by the change of workfunction of the vacuum chambers due to the chemisorption of oxygen. The electron kinetic energy distributions are calibrated with the known spectrum of the Cu^- anion and are subtracted from the photon energies to obtain the presented electron binding energy spectra.

3. Results and discussion

The photoelectron spectra of AlO^- are shown in Fig. 2 at detachment energies of 3.49 eV (355 nm) and 4.66 eV (266 nm). One major feature is observed at 355 nm with two minor features at each side of the main feature, corresponding to vibrational excitations. At 266 nm, one more well-resolved vibrational progression is revealed at higher binding energies, representing the first excited state of AlO. Fig. 3 displays the PES spectrum of AlO_2^- at 266 nm. Only one well-resolved vibrational progression is observed at quite high binding energy, indicating that AlO_2 has a very high electron affinity. Indeed, little electron signal was observed when the 355 nm photons were used to detach the AlO_2^- beam. In the following, we will discuss each molecule separately.

3.1. AlO^-

The electronic structure of AlO is well understood [17–21]. Therefore, it is rather straight forward to assign the PES spectra shown in Fig. 2. The valence molecular orbital configuration of AlO can be written as $2\sigma^2 1\pi^4 3\sigma^1$, where the 2σ and 1π orbitals are bonding orbitals mainly derived from the O atom, and the 3σ orbital is a non-bonding orbital, mostly of Al 3s character. Thus, AlO neutral is open-shell with a $^2\Sigma^+$ ground state. For AlO^-, the extra electron enters the 3σ orbital, forming a closed shell ground state, $2\sigma^2 1\pi^4 3\sigma^2$ ($^1\Sigma^+$). This is isoelectronic with SiO. Therefore, a fairly high EA is expected for AlO.

Detachment of a 3σ electron results in the ground state of the AlO neutral, responsible for the features observed at 355 nm. The peak labeled as "HB" at 2.5 eV is from a hot band transition due to the thermal vibrational excitation in the AlO^- anion. The observation of little vibrational excitation suggests that there is almost no geometry change upon removing the 3σ electron. This is consistent with the non-bonding nature of the 3σ orbital. From this

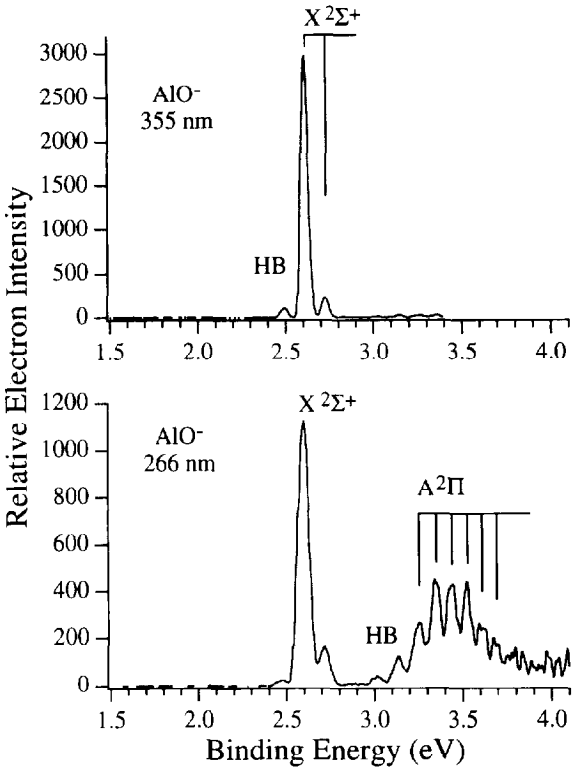

Fig. 2. Photoelectron spectra of AlO^- at 3.49 eV (355 nm) and 4.66 eV(266 nm) photon energies. Resolved vibrational features are indicated with vertical lines. "HB" stands for hot band transitions.

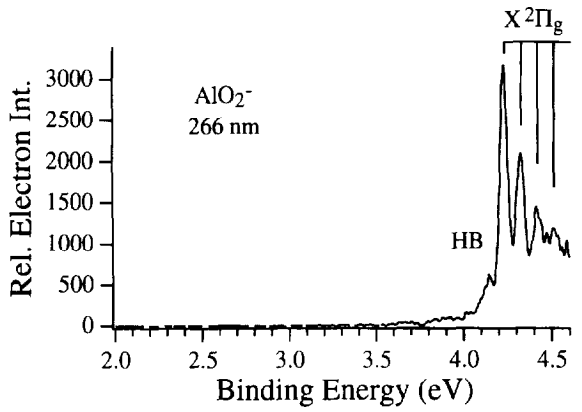

Fig. 3. Photoelectron spectrum of AlO_2^- at 4.66 eV(266 nm) photon energy. Resolved vibrational features are indicated with vertical lines. "HB" stands for hot band transitions.

spectrum, we derive the EA of AlO to be 2.60 (1) eV, and a vibrational frequency of 960 (30) cm^{-1} for the ground state, in excellent agreement with previous optical measurements [14–18]. From the resolved hot band transition, the vibrational frequency for the AlO^- anion is obtained to be 900 (50) cm^{-1}. The lower vibrational frequency for the AlO^- anion implies that the 3σ orbital is of slightly anti-bonding character. A previous calculation obtained an EA value for AlO to be 3.1 eV, which is apparently too high [21]. A vibrational frequency of 924 cm^{-1} obtained from the same work for AlO^- is in good agreement with our measurement.

Removal of a 1π electron yields the broad vibrational progression at the higher binding energy observed in the 266 nm spectrum. This corresponds to the $^2\Pi$ excited state of AlO. It is known that the $^2\Pi$ state has a spin-orbit splitting of about 130 cm^{-1} [17], which cannot be resolved in the current experiment and results in a broadening factor in each vibrational feature. This part of the spectrum is also complicated by the hot band transitions that can be easily identified because of the difference in the vibrational frequencies between the anion and the neutral. The 0–0 transition lies at the third peak as labeled in Fig. 2. The derived vibrational frequency for the $^2\Pi$ state is 700 (50) cm^{-1} and the excitation energy relative to the $^2\Sigma^+$ ground state is 0.66 eV. Both of these are in good agreement with known values [17]. The lower vibrational frequency and the broad vibrational progression are in agreement with the fact that the 1π orbital is a bonding orbital. The derived spectroscopic information for AlO and AlO^- are listed in Table 1.

3.2. AlO_2^-

From previous matrix experiments [15,16,22,23], two isomers have been observed for AlO_2: one involves a cyclic AlO_2 resembling a Al(O2) complex, and another one is the linear OAlO dioxide. The most recent calculations predict that these two isomers have nearly equal stability with the linear one slightly favored

Table 1
Observed spectroscopic constants for AlO, AlO^-, AlO_2, and AlO_2^-

		BE (eV)[a]	EA (eV)[b]	Term value (eV)		Vib. freq. (cm^{-1})	
				This work	Ref. [17]	This work	Ref. [17]
AlO	X $^2\Sigma^+$	2.60 (1)	2.60 (1)	0	0	960 (30)	979.23
	A $^2\Pi$	3.26 (2)		0.66 (2)	0.662	700 (50)	728.5
AlO^-	X $^1\Sigma^+$					900 (50)	
AlO_2	X $^2\Pi_g$	4.23 (1)	4.23 (1)	0		750 (40)[c]	
AlO_2^-	X $^1\Sigma_{g^+}$					680 (60)[c]	

[a] Adiabatic binding energy.
[b] Adiabatic electron affinity which is equal to the adiabatic binding energy of the ground state.
[c] Vibrational frequency for the totally symmetric mode.

[25]. These two isomers have quite different vibrational properties with widely different frequencies. They should also have very different electronic properties. The linear isomer should be isoelectronic with SiO_2^+ and represents a further oxidation of the Al atom relative to AlO. Thus, the anion of the linear OAlO molecule should be closed shell and isoelectronic with the SiO_2 molecule. A fairly high EA is expected for the linear isomer. On the other hand, the AlO_2 cyclic isomer with an O–O bond is in reality an $Al(O_2)$ complex. A much lower EA is expected for such a complex. A similar situation is present for the CuO_2 case, where there exist two isomers: the linear OCuO isomer has a very high EA while the $Cu(O_2)$ complex has an EA value only slightly higher than that of the Cu atom [11].

The spectrum of AlO_2^- shown in Fig. 3 represents an unusually high EA (4.23 eV) for AlO_2, compared with the EA of Al atom (0.44 eV) [28]. This spectrum reveals a simple vibrational progression with a vibrational frequency of 750 (40) cm^{-1}. From the hot band transition, a vibrational frequency of 680 (60) cm^{-1} is obtained for the AlO_2^- anion. Since only totally symmetric modes are allowed in photodetachment, the observed vibrational frequencies are most likely due to the totally symmetric ν_1 mode. The previously observed ν_1 frequency from the matrix experiments is 635 cm^{-1} for the linear OAlO while the frequency for the cyclic isomer is 1096 cm^{-1}. Our observed frequency is apparently closer to that of the linear isomer. However, there is a large discrepancy between the current value and the value reported from the matrix experiments. The discrepancy may be due to several possibilities, i.e., the matrix effect, a different vibrational mode or different isomers in the matrix experiments. The very high EA observed in our experiment is consistent with the linear isomer. Furthermore, the vibrational progression shown in Fig. 3 is along the Al–O stretching coordinate. There is no substantial excitation due to the bending mode that is expected to have a low frequency. This suggests that there is little geometry change along the bending mode between the AlO_2^- anion and AlO_2 neutral and they both have the linear equilibrium geometry. This is further confirmed by an extensive recent ab initio calculation which predicts that both AlO_2^- and AlO_2 are linear and yields vibrational frequency and electron affinity in excellent agreement with our measured values [29]. The obtained spectroscopic information from the current experiment is tabulated in Table 1.

Cyclic isomer for AlO_2^- is apparently not formed under our experimental conditions. This is understandable due to the rather high temperature plasma conditions in the laser vaporization source. It should be pointed out that when much higher laser pulse energy is used to detach the AlO_2^- beam at 355 nm very weak photoelectron signals can be observed when accumulated for a much longer time. The feeble and diffuse electron signals extended down to about 1 eV binding energy are possibly due to the scarce AlO_2^- cyclic isomer. Unfortunately, we cannot obtain more definitive information because of the extremely low abundance of this isomer. We estimate that the cyclic isomer is populated at less than 1% compared to the linear isomer under our experimental conditions.

4. Conclusions

Vibrationally resolved photoelectron spectra of AlO^- and AlO_2^- are reported. The photodetachment technique is shown to yield definitive and complementary spectroscopic information on species traditionally studied by low temperature matrix techniques. The electron affinities and vibrational frequencies of both the neutral and anions are obtained. In the case of AlO, the obtained spectroscopic constants are in good agreement with previous optical measurements. AlO_2 is observed to have a very high electron affinity and is concluded to have a linear OAlO structure.

Acknowledgements

We wish to thank Dr. K.A. Peterson for valuable discussions. This work is supported by The US Department of Energy, Office of Basic Energy Sciences, Chemical Science Division and is conducted at Pacific Northwest National Laboratory that is operated for the US Department of Energy by Battelle under Contract DE-AC06-76RLO 1830.

References

[1] L.S. Wang, H.S. Cheng and J. Fan, J. Chem. Phys., 102 (1995) 9480.
[2] K.M. Ervin, J. Ho and W.C. Lineberger, J. Chem. Phys., 89 (1988) 4514.
[3] K.M. McHugh, J.G. Eaton, G.H. Lee, H.W. Sarkas, L.H. Kidder, J.T. Snodgrass, M.R. Manaa and K.H. Bowen, J. Chem. Phys., 91 (1989) 3792.
[4] S.M. Casey and D.G. Leopold, J. Phys. Chem., 97 (1993) 816.
[5] O. Cheshnovsky, S.H. Yang, C.L. Pettiette, M.J. Craycraft and R.E. Smalley, Rev. Sci. Instrum., 58 (1987) 2131.
[6a] G. Gantefor, K.H. Meiwes-Broer, H.O. Lutz, Phys. Rev. A. 37 (1988) 2716.
[6b] C.-Y. Cha, G. Gantefor and W. Eberhardt, Rev. Sci. Instrum., 63 (1992) 5661.
[7] T.N. Kitsopoulos, C.J. Chick, Y. Zhao and D.M. Neumark, J. Chem. Phys., 95 (1991) 1441.
[8] H. Wu, S.R. Desai and L.S. Wang, Phys. Rev. Lett., 76 (1996) 212.
[9] J. Fan, J.B. Nicholas, J.M. Price, S.D. Colson and L.S. Wang, J. Am. Chem. Soc., 117 (1995) 5417.
[10] J.B. Nicholas, J. Fan, H. Wu, S.D. Colson and L.S. Wang, J. Chem. Phys., 102 (1995) 8277.
[11] H. Wu, S.R. Desai and L.S. Wang, J. Chem. Phys., 103 (1995) 4363.
[12] L.S. Wang, H. Wu, S.R. Desai and L. Lou, Phys. Rev. B, 53 (1996) 8028.
[13] H. Wu, S.R. Desai and L.S. Wang, J. Am. Chem. Soc., 118 (1996) 5296.
[14] S.J. Bares, M. Haak and J.W. Nibler, J. Chem. Phys., 82 (1985) 670.
[15] S.M. Sonchik, L. Andrews and K.D. Carlson, J. Phys. Chem., 87 (1983) 2004.
[16] L. Andrews, T.R. Burkholder and J.T. Yustein, J. Phys. Chem. 96 (1992) 10182.
[17] K.P. Huber and G. Herzberg, in: Molecular Spectra and Molecular Structure IV. Constants of Diatomic Molecules, Van Nostrand Reinhold, New York, 1979.
[18] J.P. Towle, A.M. James, O.L. Bourne and B. Simard, J. Mol. Spectrosc., 163 (1994) 300.
[19] B.H. Lengsfield III and B. Liu, J. Chem. Phys., 77 (1982) 6083.
[20] A. Marques, M.J. Capitan, J.A. Odriozola and J.F. Sanz, Int. J. Quant. Chem., 52 (1994) 1329.
[21] K.A. Peterson and R.C. Woods, J. Chem. Phys., 90 (1989) 7239.
[22] L.V. Serebrennikov, S.B. Osin and A.A. Maltsev, J. Mol. Struct., 81 (1982) 25.
[23] L.V. Serebrennikov and A.A. Maltsev, Vestnik Mosk. Univ. Khim., 26 (1985) 137.
[24] J. Rubio, J.M. Ricart and F. Illas, J. Comput. Chem., 9 (1988) 836.
[25] A.V. Nemukhin and J. Almlof, J. Mol. Struct. (Theochem), 253 (1992) 101.
[26] W.A. de Heer and P. Milani, Rev. Sci. Instrum., 62 (1991) 670.
[27] P. Kruit and F.H. Read, J. Phys. E: Sci. Instrum., 16 (1983) 313.
[28] C.S. Feigerle, R.R. Corderman and W.C. Lineberger, J. Chem. Phys., 74 (1981) 1513.
[29] K.A. Peterson, private communication.